Stanford Exploration Project, Report 67, January 13, 1998, pages 1–67

An ambient noise dataset from a producing field

Steve Cole & Leonid Vanyan[1]

keywords: *noise, sources*

ABSTRACT

We have recently begun looking at an interesting dataset where ambient seismic noise was recorded using a 480 channel array of buried geophones in a producing field. Pumps provide strong, broadband coherent energy. Using techniques that we have applied to other ambient noise datasets, we hope to locate sources of noise on the surface and at depth, and infer some details about the subsurface.

INTRODUCTION

Recently we obtained a new dataset where ambient noise was recorded in a producing oilfield, using a 480 channel array of geophones, each buried 30 feet down a borehole. These data were recorded by Unocal in Wyoming, during conventional 3-D surveys they were conducting to study the producing reservoir.

There is a great deal of strong, coherent energy in the ambient noise records. For the most part, this energy is due to pumps, which are located throughout the survey area. The noise covers a wide range of frequencies, from roughly 20 to 100 Hertz.

The pumps are strong surface noise sources, but we are interested in finding sources at depth. There are two possibilities. One is that we will be able to see secondary sources, structures in the subsurface that scatter pump noise energy. Another possibility is that seismic energy will be generated at depth due to the extraction of oil from the reservoir. In either case, the passive seismic processing methods we have previously developed for other datasets (Vanyan and Cole, 1990; Cole et al, 1989) may be useful.

Our principal processing methodology has been to look for evidence of sources at depth by summing along hyperbolic (for nearby sources) or linear (for more distant sources) trajectories. In the case of near-field sources, a 3D grid of possible source locations is constructed. Then, given an estimate of the velocity field, moveout trajectories are computed for sources at each of the grid locations. Finally the data are stacked or semblance is computed along these trajectories. This technique was first proposed by Nikolaev and Troitskiy (1987).

[1]**email:** not available

We supplemented this method in SEP–65 with a technique to suppress surface noise sources that might otherwise obscure buried sources. We will undoubtedly want to apply this technique to these data, where there are strong sources of noise on the surface.

DATASET OVERVIEW

Figure 1 shows a plan view of the survey area. Coordinates are in feet. The dots indicate receiver locations. There are twelve lines, each containing 40 geophones, with an inline spacing of 50 feet and a crossline spacing of 150 feet. The geophones are cemented in place 30 feet below the surface.

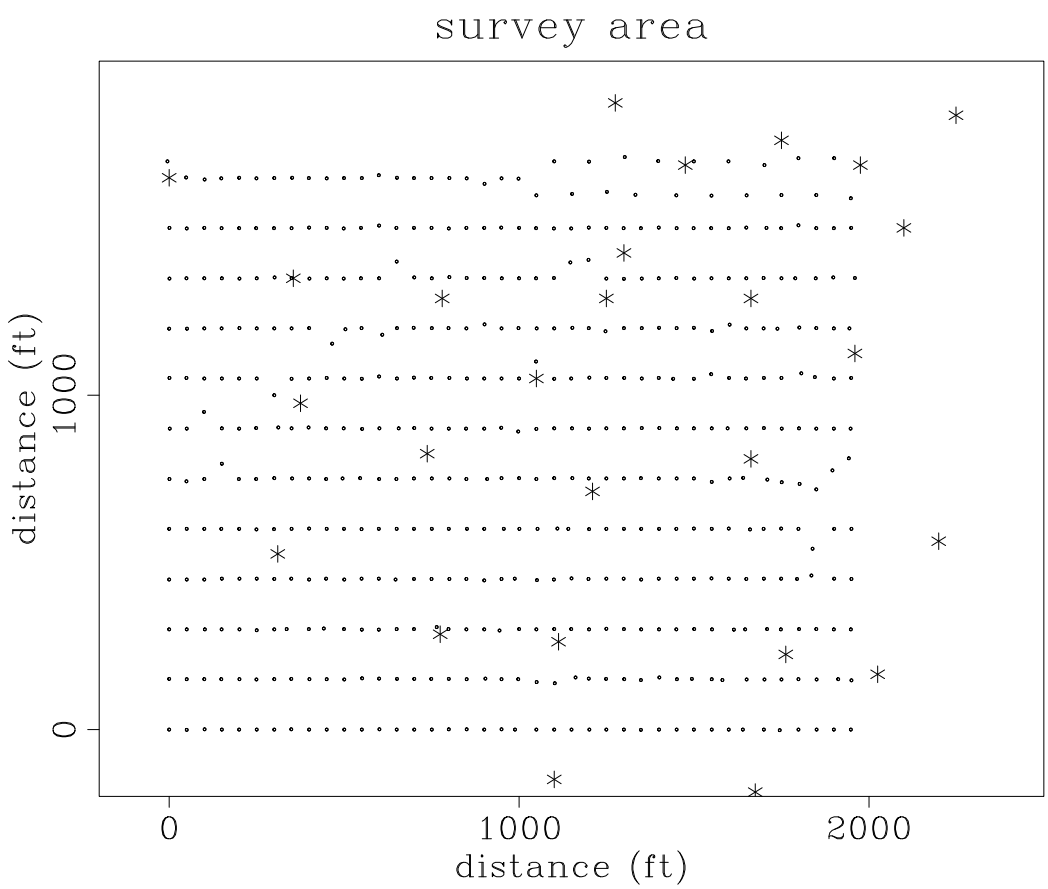

Figure 1: Plan view of survey area. Dots indicate geophone locations. Asterisks denote locations of pumps. Roughly half the pumps are operating at any given time. steve1-map [NR]

The asterisks indicate the locations of pumps. There are 26 pumps either within the boundaries of the array or close by. About half of these are operating at any time. The pumps produce strong noise that is fairly broadband, from roughly 20 to 100 Hertz, but the resonant frequency of the geophones (28 Hz) was chosen to minimize the effect of pump noise.

To date we have obtained just a few noise records, each roughly 17 seconds long. These records were obtained during a 3-D survey conducted last year. Additional noise records were taken during another 3-D survey this summer. An interesting new development in the field is that in the intervening year, a steam injection program has begun. When we look at the data from this year's survey perhaps we will notice changes in the ambient noise field due to steam injection.

Figure 2 is another plan view, this time limited to the bounds of the array, where the rms amplitudes of the traces for part of one record have been computed and plotted. The largest values are white. Superimposed on this plot are the known pump locations. Not surprisingly, the largest amplitudes are recorded near pumps.

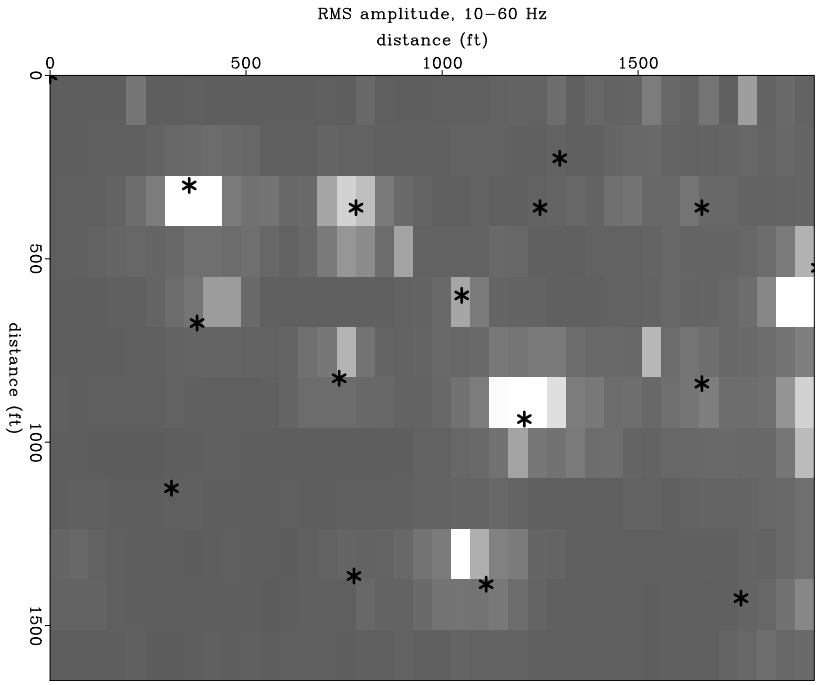

Figure 2: Plan view of array showing rms amplitudes of traces for a 2 second portion of one record. Superimposed on this plot are the pump locations that lie within the receiver array. The strongest amplitudes are measured near working pumps. Some pumps were not working during this interval. steve1-rms [NR]

Figure 3 shows the data from three lines of the array. They are the third, sixth, and tenth lines counting up from the bottom of Figure 2. Each of these lines has at least one active pump on the line or nearby, and the energy from the pumps is clearly visible on the displays. For example, in Figure 2 we see that line 3 has a pump near its center. In the left plot of Figure 3, we see a burst of energy from this pump beginning at around 0.5 seconds. Trace balancing has been used to compensate for the decrease in amplitudes away from the pumps, and these panels have been bandpass filtered to 10-60 Hz.

In Figure 4, the data have also been filtered using a 3-D recursive dip filter. The coherency of the pump noise events is clearer after this filtering.

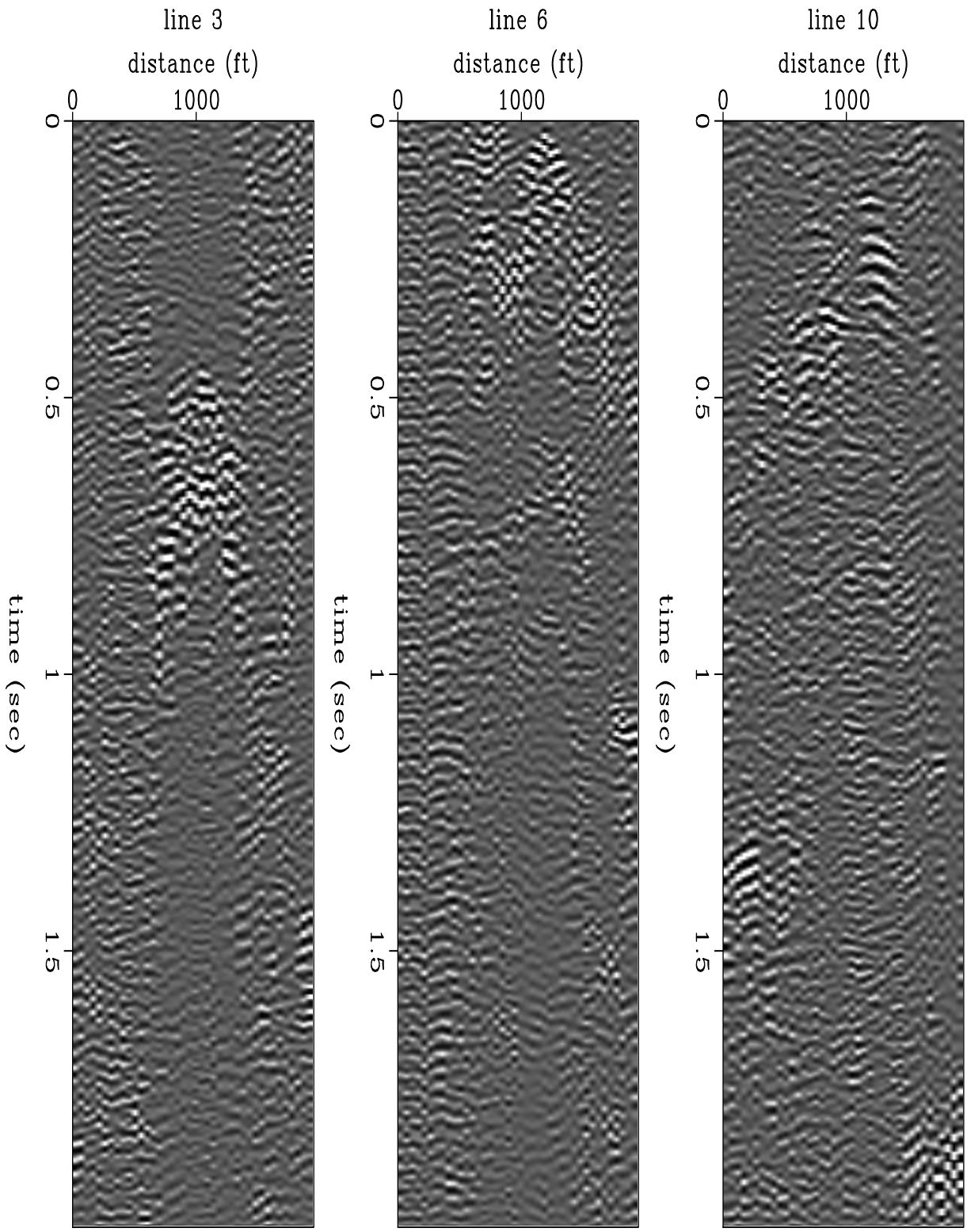

Figure 3: Data from three of the twelve receiver lines. Bursts of energy from pumps is clearly visible on all three profiles, and the locations can be tied to Figure 2. steve1-data [NR]

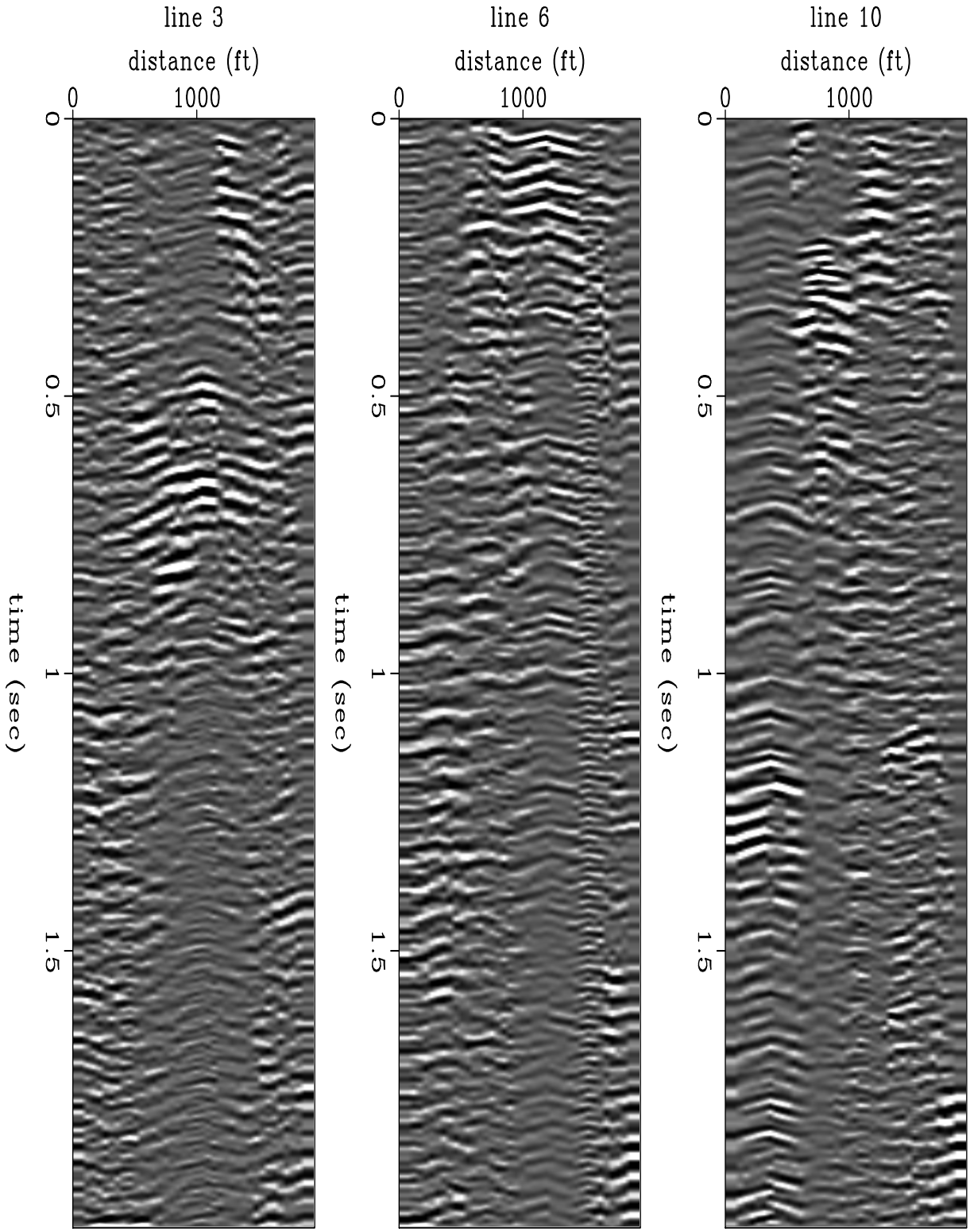

Figure 4: Data from three of the twelve receiver lines (same as Figure 3), but in this display the data have also been 3-D dip filtered. The pump noise events are easier to distinguish. steve1-datadip [NR]

Figure 5 shows the amplitude spectra for line 3, the line on the left in Figure 3. The pump energy has a fairly broad spectrum, with abundant energy from 20 to 100 Hertz.

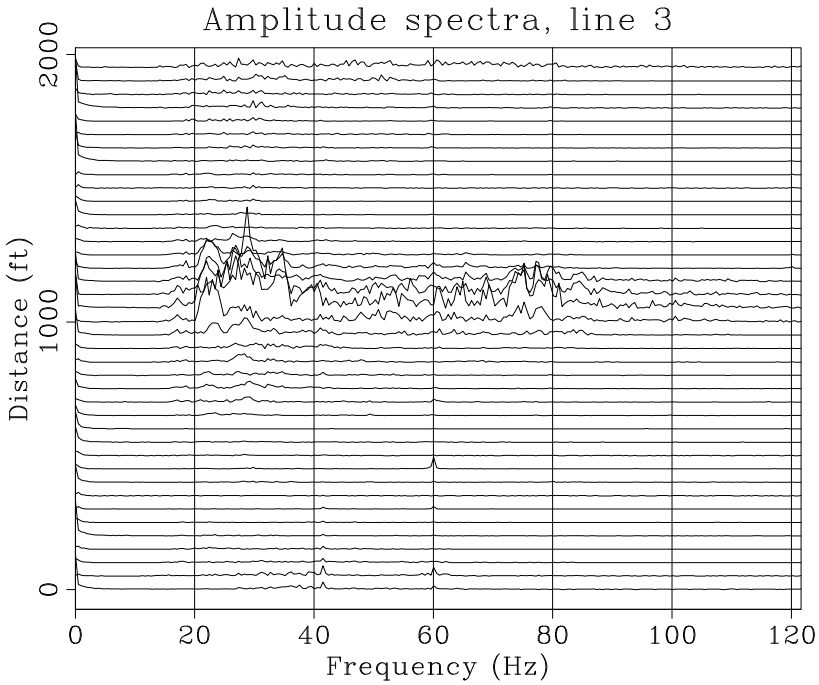

Figure 5: Spectra for line 3 from Figure 3. Pump noise energy extends beyond 100 Hz. steve1-spec [NR]

SEMBLANCE COMPUTATION

It is clear that there are energy sources, at least on the surface, in the dataset. We would now like to search for sources at all depths. To do this, we construct a 3-D grid of possible source locations. Then, given an estimate of the velocity structure, we compute the moveout trajectory for energy coming from each source location, and use the data to compute semblance along these trajectories.

We performed these computations for two frequency ranges, a low-frequency (10-60 Hz) band, within which we expected pump noise to dominate, and a higher-frequency band (40-120 Hz) in which we hoped that pump noise wouldn't dominate and we would see energy from other sources, perhaps energy generated at the depth of the reservoir by the extraction of oil.

Figures 6 and 8 show the results of the semblance computations for the low-frequency range for two different records. The different panels show the semblance as a function of x and y for various depths. The limits of each panel are the boundaries of the array. The main feature of these plots is high semblance values at shallow depths. These values correspond to pump noise.

Figures 7 and 9 show the maximum value of semblance (for all x and y) as a function of depth. These plots confirm the conclusion that the main sources of energy in the low frequency range are on the surface.

The results are quite different for the high-frequency range, however. Figures 10 and 12 show the semblance results for the two records. For depths less than approximately 350 meters, the patterns are rather random, but become more organized as depth increases. The graphs of maximum semblance versus depth (Figures 11 and 13) show that semblance increases at a depth of around 700 meters for record 1 and 400-600 meters for record 2. This may be evidence for sources of energy other than pump noise occurring at depth. Perhaps it is energy generated by the reservoir during the process of oil extraction.

CONCLUSIONS

The initial results are promising. Pumps are strong surface sources that are easy to locate. There seems to be some evidence of sources at depth if we take the right frequency band. We may do a better job at uncovering such sources if we suppress surface sources as we have done in other work.

ACKNOWLEDGMENTS

We would like to thank Unocal for providing the dataset. In particular we want to thank Phil Johnston for his assistance.

REFERENCES

Cole, S., Claerbout, J.F., Nichols, D., and Zhang, L., 1989, The ambient seismic field in three dimensions: Presented at the 59th Ann. Int'l. Mtg., Soc. Expl. Geophys.

Nikolaev, A.V., and Troitskiy, P.A., 1987, Lithospheric studies based on array analysis of P-coda and microseisms: Tectonophysics **140**, 103-113.

Vanyan, L., and Cole, S., 1990, Comparison of different approaches to processing ambient noise data: SEP–**65**, 191-208.

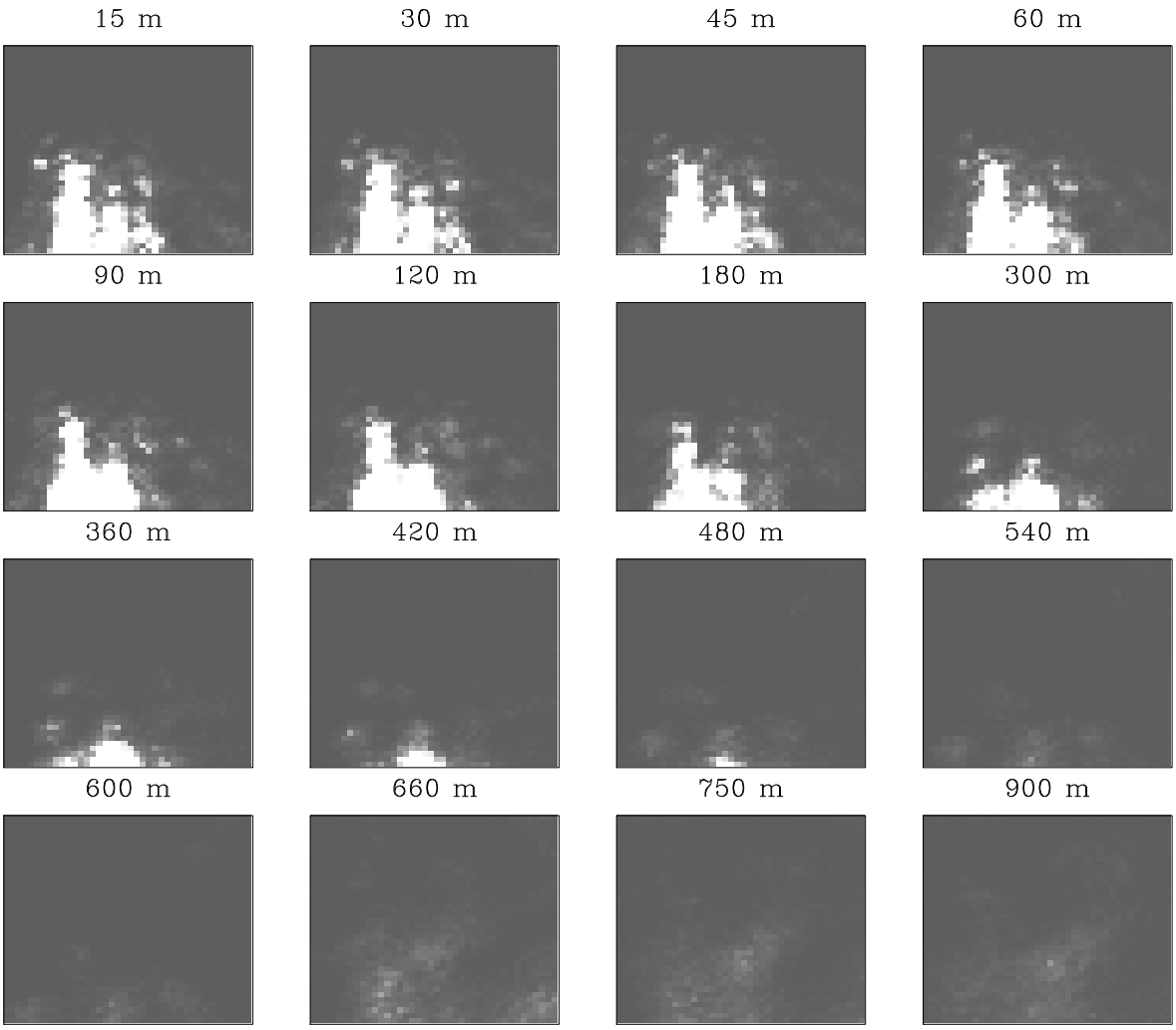

Figure 6: Semblance computed along moveout trajectories for possible source locations in 3-D. Each panel corresponds to a different depth. The limits of each picture are the boundaries of the array. Data in the low-frequency range (10-60 Hz) were used, and not surprisingly noise from pumps on the surface dominates the results. steve1-l1 [NR]

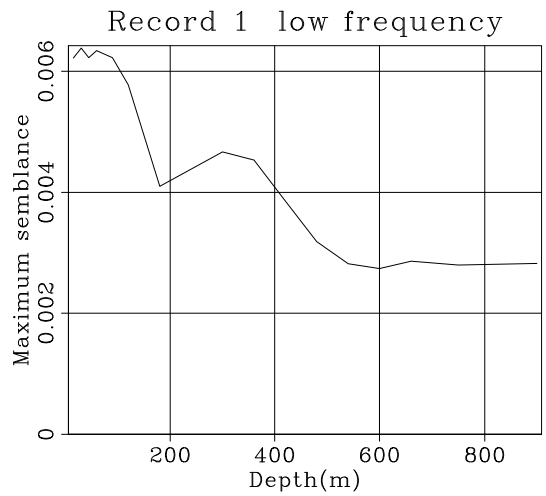

Figure 7: Maximum value of semblance from Figure 6 as a function of depth. Verifies that surface sources dominate. steve1-gl1 [NR]

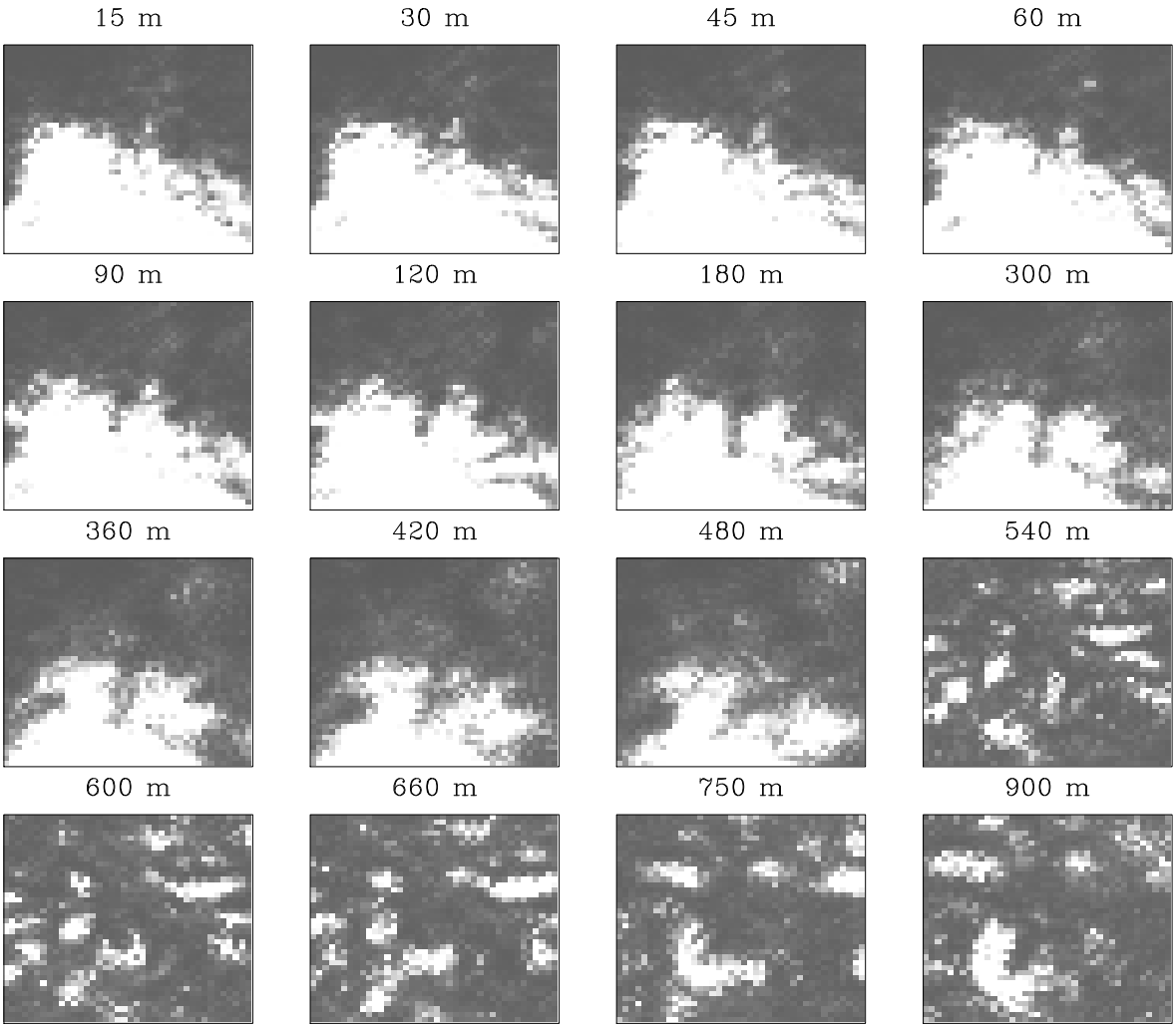

Figure 8: Same semblance computation in 3-D as Figure 6, but for record 2. Surface noise sources dominate again. steve1-l2 [NR]

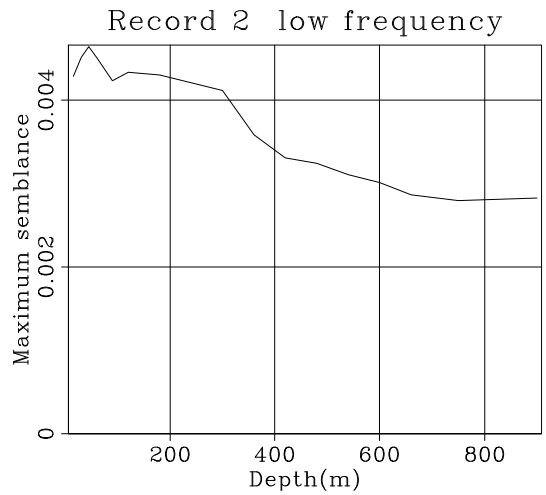

Figure 9: Maximum value of semblance vs. depth for Figure 8. Surface sources are not as dominant as in record 1. steve1-gl2 [NR]

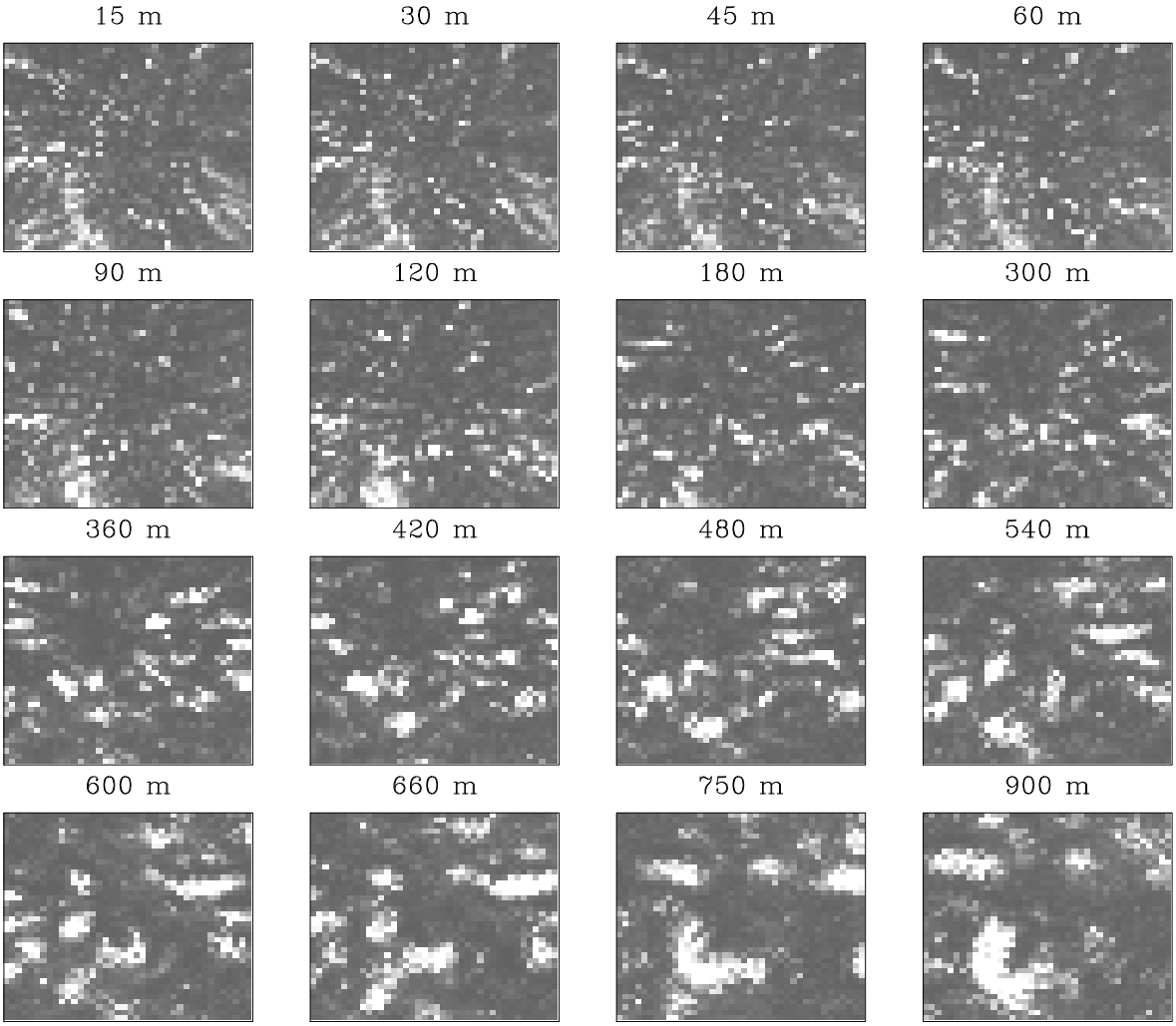

Figure 10: Semblance computation in 3-D for record 1, using the high frequency range (40-120 Hz) over which pump noise is less dominant. Unlike the low-frequency case (Figure 6), here there are large semblance values at depth. steve1-h1 [NR]

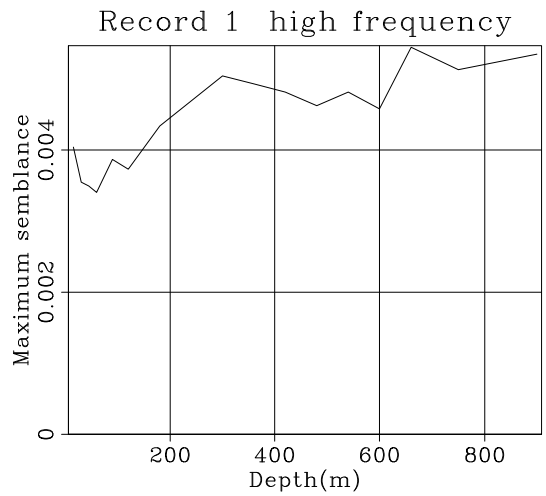

Figure 11: Maximum value of semblance as a function of depth for Figure 10. Note the increase at around 700 meters, suggesting that non-surface sources are present. steve1-gh1 [NR]

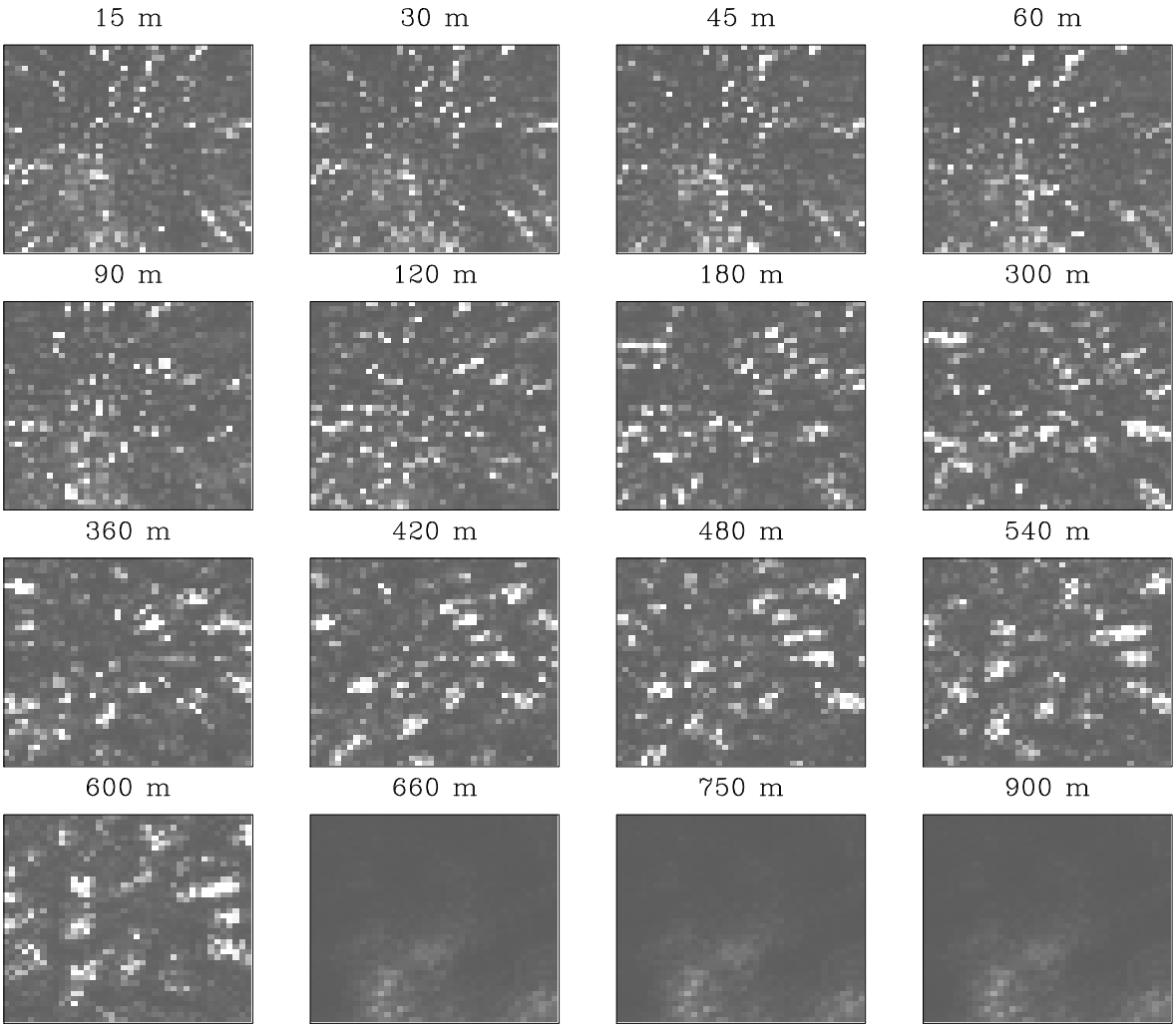

Figure 12: Same semblance computation as Figure 10, but for record 2. steve1-h2 [NR]

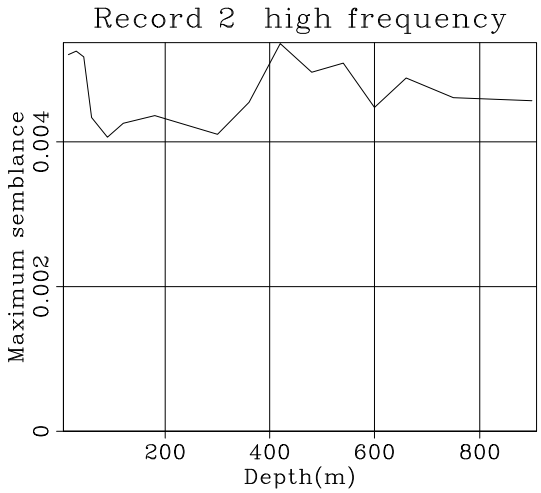

Figure 13: Maximum value of semblance vs. depth for Figure 12. Here also there is a semblance increase at depth. steve1-gh2 [NR]